



CO₂ flux geothermometer for geothermal exploration

M.C. Harvey^{a,*}, J.V. Rowland^a, G. Chiodini^b, C.F. Rissmann^c, S. Bloomberg^d,
T. Fridriksson^e, A.A. Oladottir^e

^a School of Environment, University of Auckland, Auckland, New Zealand

^b Istituto Nazionale di Geofisica e Vulcanologia sezione di Bologna "Osservatorio Vesuviano", Via Diocleziano, Napoli 328-80124, Italy

^c GNS Science, New Zealand

^d Department of Geology, Mines, and Water Resources, Private Bag PMB001, Port Vila, Vanuatu

^e Iceland GeoSurvey, Grensasvegur 9, 108 Reykjavik, Iceland

Received 12 September 2016; accepted in revised form 17 June 2017; Available online 23 June 2017

Abstract

A new geothermometer ($T_{\text{CO}_2 \text{ Flux}}$) is proposed based on soil diffuse CO₂ flux and shallow temperature measurements made on areas of steam heated, thermally altered ground above active geothermal systems. This CO₂ flux geothermometer is based on a previously reported CO₂ geothermometer that was designed for use with fumarole analysis. The new geothermometer provides a valuable additional exploration tool for estimating subsurface temperatures in high-temperature geothermal systems. Mean $T_{\text{CO}_2 \text{ Flux}}$ estimates fall within the range of deep drill hole temperatures at Wairakei (New Zealand), Tauhara (New Zealand), Rotokawa (New Zealand), Ohaaki (New Zealand), Reykjanes (Iceland) and Copahue (Argentina). The spatial distribution of geothermometry estimates is consistent with the location of major upflow zones previously reported at the Wairakei and Rotokawa geothermal systems. $T_{\text{CO}_2 \text{ Flux}}$ was also evaluated at White Island (New Zealand) and Reporoa (New Zealand), where limited sub-surface data exists. Mode $T_{\text{CO}_2 \text{ Flux}}$ at White Island is high (320 °C), the highest of the systems considered in this study. However, the geothermometer relies on mineral–water equilibrium in neutral pH reservoir fluids, and would not be reliable in such an active and acidic environment. Mean $T_{\text{CO}_2 \text{ Flux}}$ at Reporoa (310 °C) is high, which indicates Reporoa has a separate upflow from the nearby Waiotapu geothermal system; an outflow from Waiotapu would not be expected to have such high temperature.

© 2017 Elsevier Ltd. All rights reserved.

Keywords: CO₂; Flux; Geothermometer; Shallow; Temperature

1. INTRODUCTION

During the last five decades, various liquid and gas phase chemical geothermometers have been successfully utilised to estimate temperatures in geothermal reservoirs (Arnórsson and Gunnlaugsson, 1985; Fournier, 1977; Giggenbach, 1980; Henley et al., 1984; Giggenbach, 1988; Chiodini and Marini, 1998). The liquid geothermometers are based on the concentrations of dissolved chemical spe-

cies present in thermal waters from thermal springs and shallow drillholes. Accordingly, they may only be used when deeply sourced thermal waters flow into drill holes or can be sampled from surface springs. It is important that waters discharged from springs have ascended quickly enough from the reservoir to avoid re-equilibration. Similarly, gas geothermometers require the presence of fumaroles; naturally occurring point sources of high pressure vapour discharge.

Springs are often of the acid-sulphate variety, essentially steam-heated near surface meteoric waters. Such waters contain little of the original chemical information and are

* Corresponding author.

E-mail address: mhar098@aucklanduni.ac.nz (M.C. Harvey).

not useful for geothermometry. Even deeply sourced spring waters are subject to dilution, or may undergo geochemical re-equilibration along their flow paths. Such waters may provide geothermometry, but only where sufficient samples can be obtained to allow the construction of mixing models, and to determine the derivation of parent waters (Fournier, 1977; Arnórsson, 1985).

These limitations are similar for gas geothermometry. For gas samples to be reliable the fumarole discharge should be hot and vigorous (Arnórsson et al., 2006). Samples collected from weak fumaroles may be contaminated because of the sampling method (evacuated glass flask); the vacuum may draw air into the flask during sampling. Even where contamination can be prevented, fumaroles are often subject to condensation of water vapour, leading to enrichment of the non-condensable gas components in the sample. The effect of condensation is in one sense a problem of sample size, analogous to the problem of dilution in spring water geothermometry; in theory, both problems can be overcome if a sufficient number of samples can be collected to allow mixing/condensation models to be built.

In contrast to the scarcity of suitable springs and fumaroles, areas of steam heated ground are much more common. This paper explores a new method that allows a practically unlimited number of gas concentration (CO₂) estimates to be made in areas of steam heated ground. The method provides for using large datasets that can be interpreted by previously reported CO₂ geothermometers (Giggenbach, 1984; Arnórsson and Gunnlaugsson, 1985). The principle of these geothermometers is that the concentration of CO₂ in a high temperature, liquid geothermal reservoir is controlled by temperature dependent mineral–water equilibrium of the general form: Plagioclase + CO₂ = Clay + Calcite (Giggenbach, 1981). This study considers eight geothermal fields: six in the Taupō Volcanic Zone (TVZ), New Zealand, one in Iceland (Reykjanes) and one in Argentina (Copahue). In the TVZ, the most common primary form of plagioclase is andesine (Browne and Ellis, 1970; Steiner, 1977), with clay minerals ranging from smectite (montmorillonite), through mixed-layer clays to chlorite and illite (Harvey and Browne, 1991). In Iceland, the concentration of CO₂ in basalt-hosted reservoir fluids above 230 °C is controlled by the reaction: Prehnite + CO₂ = Epidote + Calcite (Arnórsson et al., 1998; Stefánsson and Arnórsson, 2002). The Copahue volcano produces a mixture of andesitic to basaltic–andesitic pyroclastics and lava flows (Agusto et al., 2013), so a similar set of mineral–water reactions are expected to control the concentration of CO₂.

The empirical CO₂ geothermometer of Arnórsson and Gunnlaugsson (1985) was originally intended to estimate deep reservoir temperatures from CO₂ concentration in fumarole steam. The geothermometer assumes adiabatic boiling of thermal fluid from the equilibrium reservoir temperature to atmospheric pressure. This assumption allows the original CO₂/water ratio in the deep reservoir to be deduced from the CO₂/steam ratio measured in fumarole steam; deep water of a given temperature boils to atmospheric pressure with an associated steam mass fraction, a

process that gives a predictable CO₂/steam ratio in the fumarole (Arnórsson and Gunnlaugsson, 1985).

In situations where heat flow from the reservoir is not adiabatic, where secondary boiling processes occur, or where steam condensation occurs within the fumarole conduit, the geothermometer may be compromised. Evidently, Arnórsson and Gunnlaugsson (1985) had reliable fumaroles available to validate their methodology, as they observed good agreement between measured reservoir temperatures from geothermal wells, and those inferred from nearby fumaroles.

It has also been suggested that a proportion of ascending magmatic CO₂ may bypass the hydrothermal reservoir (Werner and Cardellini, 2006). In such cases, surface CO₂ flux would not provide any information relating to the reservoir (i.e. temperature). However, this situation presumably would not apply to surveys conducted on areas of steaming ground that are clearly supplied by vapour from the reservoir (i.e. this study). Alternatively, strong pulses of magmatic CO₂ might overwhelm the capacity of mineral buffers in the overlying reservoir. This could result in non-equilibrium, physical control over reservoir CO₂ concentrations and very high surface CO₂ flux.

Here, we utilize the geothermometer of Arnórsson and Gunnlaugsson (1985), but replace scarce fumarole samples with abundant measurements of CO₂ flux and shallow temperatures made on steam heated ground. We compare our results with measured and inferred deep reservoir temperatures from the study areas.

Five of the New Zealand systems (Wairakei, Tauhara, Rotokawa, Ohaaki and Reporoa) are located within an ~100 km² area of the central TVZ, one of the most productive areas of Quaternary silicic volcanism in the world (Fig. 1). The TVZ represents the southernmost ~300 km of the ~2800 km Tonga-Kermadec arc system where it terminates in the continental crust of New Zealand. At a regional scale, the TVZ contains 23 high temperature geothermal systems with a total of ~4.2 GW thermal energy release; geothermal plumes exploit tectonically maintained permeability, upflow-zones that have been widely explored by deep drilling and utilized for electricity generation (Rowland and Sibson, 2004; Wilson and Rowland, 2016). Production of geothermal fluids at Wairakei caused a pressure response in the Tauhara geothermal reservoir, about 10 km to the southeast, demonstrating the two systems are hydrologically connected at depth. Rotokawa, 10 km to the northeast, has not responded to production at Wairakei (Bixley et al., 2009). The Reporoa geothermal field is located about 10 km south of the Waioatapu system (Fig. 1). Reporoa was previously interpreted to be supplied by fluid outflowing from Waioatapu, based on shallow-penetrating resistivity data and preliminary geochemical data (Hatherton et al., 1966; Healy and Hochstein, 1973). However, a connection between Reporoa and Waioatapu was later refuted on the basis of shallow (Bibby et al., 1994) and deep (Risk et al., 1994) resistivity surveying.

The five TVZ systems are predominantly recharged by meteoric water, are located at low elevation and are not presently associated with active volcanism (Rissmann

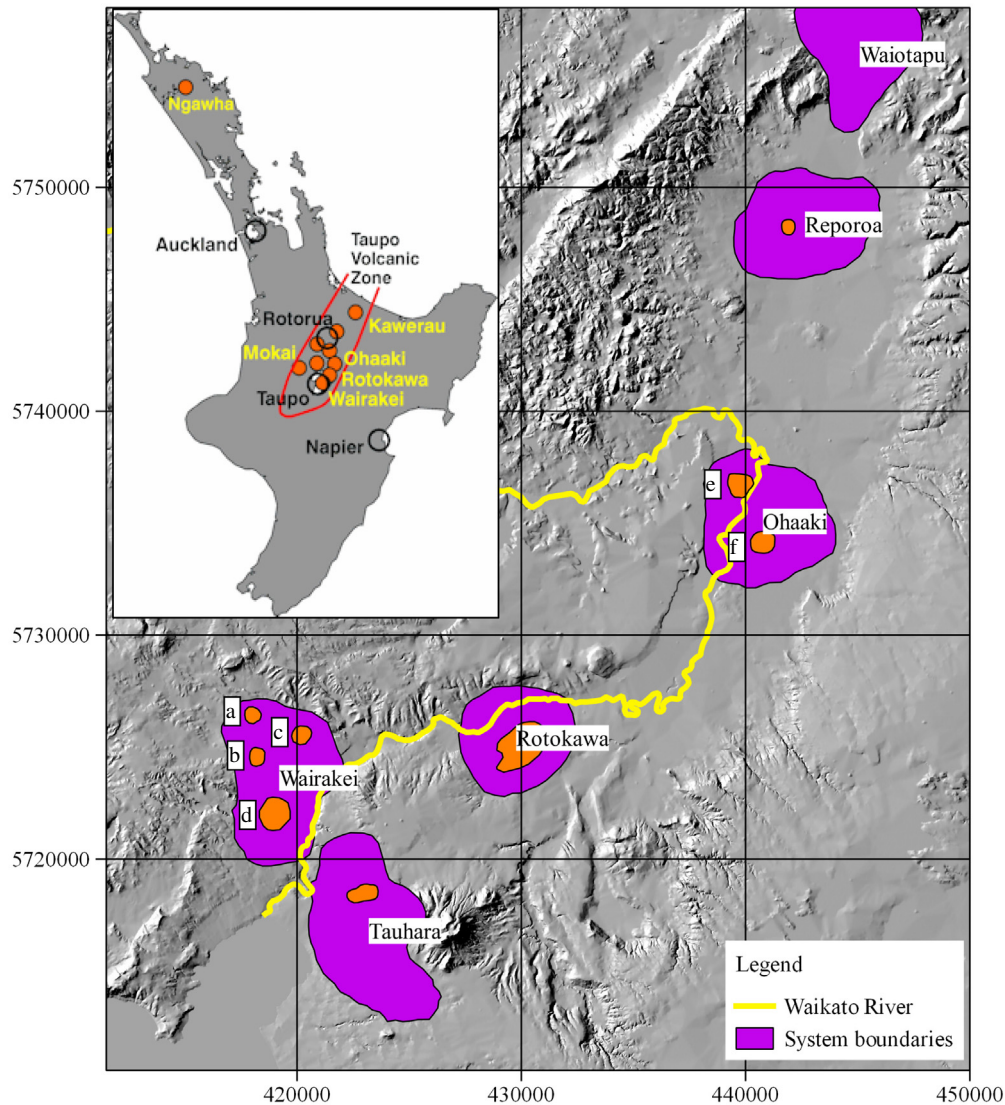


Fig. 1. Location of study areas in the Taupō Volcanic Zone overlaid on a satellite digital terrain model (WGS84). System boundaries are based on shallow electrical resistivity data (Bibby et al., 1994). Survey areas (orange) are shown within system boundaries: (a) Hot Hill, (b) Upper Waiora Valley, (c) Geyser Valley, (d) Karapiti, (e) Ohaaki West, and (f) Ohaaki East. (For interpretation of the references to colour in this figure legend, the reader is referred to the web version of this article.)

et al., 2012; Bloomberg et al., 2014; Harvey et al., 2015a). CO₂ flux and shallow temperature measurements were collected from bare and vegetated areas of thermal ground (Table 1).

Whakaari/White Island, also in the TVZ, is an active andesitic stratovolcano island located ~130 km NE along strike from the other TVZ systems. Within the crater floor of the volcano there is an active hydrothermal system which sources its fluids from seawater, magmatic, and meteoric waters (Houghton and Nairn, 1991; Gigenbach et al., 2003). CO₂ flux and shallow temperature measurements were collected from the crater floor, an area of bare thermal ground with high temperature fumaroles (>220 °C), and a large boiling acid lake which is the current site of volcanic activity (Table 1) (Bloomberg et al., 2014).

Copahue is an active Pleistocene stratovolcano located in Patagonia, Argentina, within the Copahue–Caviahue Volcanic Complex (CCVC). CO₂ flux and shallow temperature measurements were collected from bare thermal ground and wet peaty soils in four distinct areas located on the north-eastern flank the Copahue volcano (Table 1) (Chiodini et al., 2015).

The Reykjanes geothermal area is located at the south-western tip of the Reykjanes peninsula, Iceland. As with all magmatism on the mid-Atlantic ridge, the Reykjanes system produces basalt. At Reykjanes, magmatism is currently confined to the sub-surface, but occasional fissure eruptions occur at approximately 1000 year intervals. Surface activity at Reykjanes includes fumaroles, steam heated ground and mud pools (Table 1) (Fridriksson et al., 2006).

Table 1
System setting.

System	Aquifer Temp ^a (°C)	Host Rock Type ^b	Reservoir Characteristics ^c	Backgr. CO ₂ flux (g m ⁻² d ⁻¹) ^d	Exploited System ^e	Reference
Wairakei, New Zealand	240–250	Andesite-Rhyolite	Low-gas, non-magmatic, neutral	5	Yes	Giggenbach (1995), Werner et al. (2004), Glover and Mroczek (2009) and Rosenberg et al. (2009)
Tauhara, New Zealand	250–270	“	Low-gas, non-magmatic, neutral	10	Yes	Giggenbach (1995), Glover and Mroczek (2009), Rosenberg et al. (2009) and Rosenberg et al. (2010)
Rotokawa, New Zealand	<300 (intermediate)	“	High-gas, possible magmatic conditions at depth in south of field. Neutral at depth	5	Yes	Giggenbach (1995), Bloomberg et al. (2014) and McNamara et al. (2016)
Ohaaki West, New Zealand	180–310	“	High-gas, non-magmatic	15	Yes	Giggenbach (1995) and Rissmann et al. (2012)
Ohaaki East, New Zealand	240–290	“	High-gas, possible magmatic conditions at depth. Neutral	15	Yes	Giggenbach (1989), Giggenbach (1995), Christenson et al. (2002) and Rissmann et al. (2012)
Reporoa, New Zealand	Unknown	“	Unknown	10	No	Healy and Hochstein (1973) and Simpson and Bignall (2016)
White Island, New Zealand	High	Andesite	High gas, near surface magmatic conditions. Active volcano	0	No	Giggenbach (1987), Houghton and Nairn (1991), Hedenquist et al. (1993) and Giggenbach et al. (2003)
Copahue, Argentina	240–300	Basalt-Andesite	Unknown, but Magmatic conditions nearby (~6 km). Active volcano	5–26	No	Agusto et al. (2013) and Chiodini et al. (2015)
Reykjanes, Iceland	290	Basalt	Low gas, near-neutral	4	Yes	Arnórsson (1978), Fridriksson et al. (2006), Freedman et al. (2009) and Ármannsson (2016)

^a Temperature from deep well measurements (White Island is inferred).

^b From deep well cuttings and core.

^c From surface and sub-surface observations.

^d Background biological CO₂ flux estimated using statistical methods (Copahue, Reykjanes) (Chiodini et al., 1998), or ¹³CO₂ isotope analysis (New Zealand systems) (Harvey et al., 2015a,b).

^e Hydrothermal reservoir is utilized for power generation.

Hydrothermal systems were included on the basis that the temperature of the deep reservoir was known from deep drilling, or could be inferred from other data. The objective of the study is to determine if the proposed geothermometer can provide estimates of deep reservoir temperature that avoid the problems of atmospheric contamination and a limited sample size described above. Table 1 provides a summary of the physical and chemical characteristics of these systems, and references for more detailed background information.

2. METHODS

2.1. Methodology for measurement of CO₂ flux from steaming ground

Soil CO₂ flux measurements at all areas were made with an accumulation chamber type meter, an established technique for the determination of soil diffuse CO₂ flux in geothermal and volcanic areas (Brombach et al., 2001; Chiodini et al., 2005; Fridriksson et al., 2006; Hernández et al., 2012; Rissmann et al., 2012). The accumulation method calculates CO₂ flux by placing a ~200 mm diameter chamber on the soil surface and pressing it into the soil to obtain a seal. Gases flowing into the chamber are pumped through an infrared gas analyser and returned to the chamber, the increase in CO₂ concentration over time is recorded by the instrument. The rate of concentration increase is proportional to CO₂ flux (mmol m⁻² d⁻¹).

2.2. Methodology for measurement of heat flux from steaming ground: Wairakei, Tauhara and Reporoa

For each CO₂ flux measurement, soil temperatures were measured with a handheld Type-K thermocouple probe inserted to a maximum depth of 1 m below ground level. Temperatures were measured at 5–10 cm intervals, depending on the temperature gradient. Temperatures were measured at 5 cm intervals in locations with very high heat flow so depth to boiling point (for pure water at local elevation) could be more accurately measured. The probe temperature was allowed to equilibrate for at least 30 s before each reading. Two probes were used to allow cross checking of temperature measurements to verify measurement accuracy.

In order to quantify steam flux, heat flux from hot ground was first assessed by the empirical method of Hochstein and Bromley (2005). Their equation provides the total heat flux per m², incorporating both convective and conductive vapour flux:

$$Q_{\text{tot}} = \alpha(Z_{\text{bp}}/Z_o)^{-\beta} \quad (1)$$

where Q_{tot} is the total heat flux (W m⁻²), α (185 W m⁻²) and β (0.757) are empirically derived constants, Z_{bp} is the depth to boiling (for pure water at local elevation), and Z_o is the unit of depth (1 m). If the boiling temperature was not reached at 1 m depth, it was obtained by extrapolation assuming a power law or polynomial relationship, whichever gave the best curve fit. Measurements with

$Z_{\text{bp}} > 2$ m were disregarded to limit extrapolation error (Section 2.3). Eq. (1) was calibrated using a closed bottom calorimeter, and supersedes an older empirical relationship calibrated with an open bottom calorimeter (Dawson, 1964). The open bottom design had temperature stabilisation problems that gave poor data reproducibility (Bromley and Hochstein, 2005; Hochstein and Bromley, 2005).

2.3. Methodology for measurement of heat flux from steaming ground: Rotokawa, White Island, Ohaaki, Reykjanes and Copahue

Shallow temperature data from Rotokawa, White Island, Ohaaki, and Reykjanes were collected at a single depth (0.15 m). Data from Copahue, were collected at 0.1 m. Full methodology for shallow temperature measurement in these areas is provided within references (Table 1). This methodology does not provide a multi-measurement temperature profile (as were obtained at Wairakei, Tauhara and Reporoa – see Section 2.2). However, data from these areas could be used (i.e. in Eq. (1)), because of the correlation between boiling point depth, and temperature at 0.1 m and 0.15 m. This correlation was established by regressing boiling point depth on temperatures at 0.15 and 0.10 m depth using 1 m temperature profiles from Wairakei, Tauhara and Reporoa ($n = 511$) (Fig. 2a and c).

The uncertainty (scatter) of the regression is not constant, but increases with boiling point depth (Fig. 2a and c). At 2 m boiling point depth, the equivalent shallow temperature (23 °C at 0.15 m) (Fig. 2a) is close to the ambient daytime summer temperatures at Wairakei, Tauhara and Reporoa. Accordingly, only data with an estimated boiling point depth of <2 m were considered in this study.

In order to quantify the magnitude of uncertainty for various ranges of shallow temperature, we divided the Wairakei, Tauhara and Reporoa dataset into 5 °C intervals (from 40 to 100 °C), then performed a linear regression on each interval. Temperature interval was then plotted against its standard error (SE), and a curve fitted to this relationship (Fig. 2b and d).

2.4. Methodology for measurement of steam flux from steaming ground

Although Eq. (1) provides units of heat flux (W m⁻²), steam flux can be inferred by assuming the measured heat flux results from the sum of (i) condensation of steam in the shallow sub-surface (conductive heat flux), and (ii) convective steam flux (Brombach et al., 2001; Werner et al., 2004; Hochstein and Bromley, 2005; Fridriksson et al., 2006):

$$F_{\text{stm}} = Q_{\text{tot}}(h_s - h_w)^{-1} \quad (2)$$

where F_{stm} is the steam flux (kg m⁻² s⁻¹), Q_{tot} is the inferred heat flux (Eq. (1)), h_s is the enthalpy of steam at the local boiling point (kJ kg⁻¹), h_w is the enthalpy of liquid water at ambient conditions (kJ kg⁻¹).

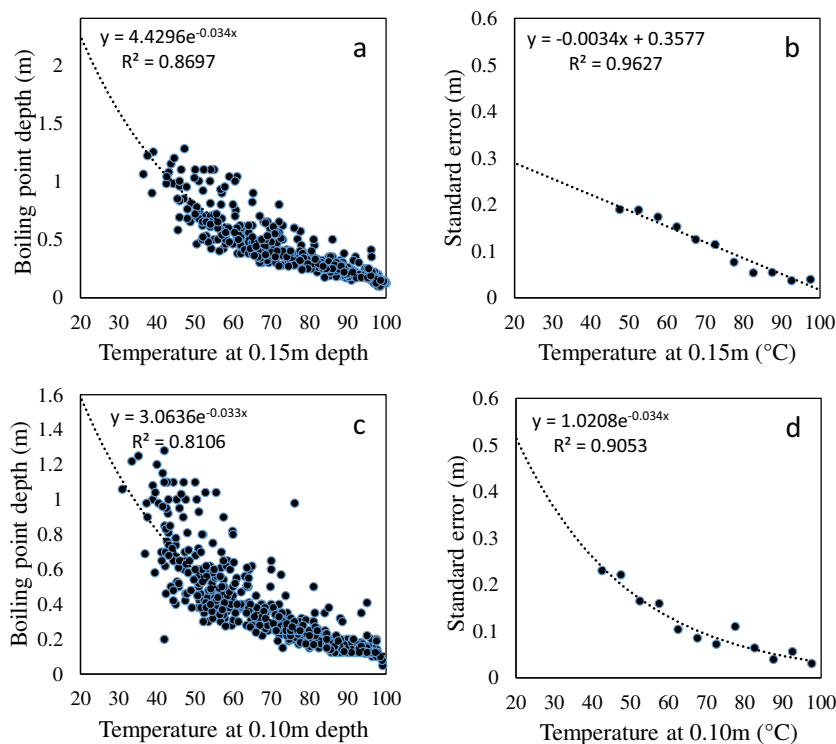


Fig. 2. Depth-to-boiling point versus temperature at 0.15 m (a), and 0.1 m depth (c). Note: scatter decreases as shallow temperature increases. Scatter (standard error) versus depth for (a) and (c) is plotted in (b) and (d), respectively.

2.5. Methodology for determination of deep reservoir temperature from $\text{CO}_2/\text{H}_2\text{O}$

The concentration of CO_2 in steam supplying the thermal area can be derived from the ratio of CO_2 flux (Section 2.1) and steam flux (Section 2.4). This approach was used previously, and found to agree with concentrations derived from fumarole gas analysis in the same area (Brombach et al., 2001; Werner et al., 2004). This concentration can then be transformed to units of temperature ($^{\circ}\text{C}$) using the CO_2 geothermometer of Arnórsson and Gunnlaugsson (1985):

$$T_{\text{CO}_2 \text{ Flux}} = -44.1 + 269.25R - 76.88R^2 + 9.52R^3 \quad (3)$$

where $T_{\text{CO}_2 \text{ Flux}}$ is the reservoir temperature ($^{\circ}\text{C}$), and R is the logarithm of the concentration of CO_2 in steam supplying the thermal area ($\log \text{ mmol kg}^{-1}$), from CO_2 flux measurements and Eq. (2). Eq. (3) is applicable to high temperature geothermal reservoirs hosted in mafic to silicic rocks (Arnórsson and Gunnlaugsson, 1985), which includes all systems in this study (Tables 1 and 2).

Alternatively, by assuming adiabatic boiling from the equilibrium reservoir temperature to atmospheric pressure (Arnórsson and Gunnlaugsson, 1985), the CO_2 geothermometer of Gigg (1984) (his Eq. 15) may be adapted in the same way:

$$T_{\text{CO}_2 \text{ Flux Gigg}} (^{\circ}\text{C}) = 51.773R + 154.04 \quad (4)$$

where $T_{\text{CO}_2 \text{ Flux Gigg}}$ is the reservoir temperature ($^{\circ}\text{C}$), and R is the logarithm of the concentration of CO_2 in steam

supplying the thermal area ($\log \text{ mmol kg}^{-1}$), from CO_2 flux measurements and Eq. (2).

$T_{\text{CO}_2 \text{ Flux}}$ (Eq. (3)) and $T_{\text{CO}_2 \text{ Flux Gigg}}$ (Eq. (4)) were compared for a range of simulated CO_2 concentrations (Fig. 3). Eq. (4) gives lower temperatures at high CO_2 concentrations, and higher temperature estimates at low CO_2 concentrations, although both give similar results ($<10^{\circ}\text{C}$ difference) between 200 and 300 $^{\circ}\text{C}$ (Fig. 3).

For simplicity, and because Eq. (3) was originally intended to estimate deep reservoir temperatures from CO_2 concentration in fumarole steam, we have utilised Eq. (3). Applying Eq. (3) to all survey measurements from an area of steaming ground transforms lognormal raw data to a normally distributed population of reservoir temperatures that can be described by standard statistical measures (mean, mode and standard deviation).

For Rotokawa, White Island, Ohaaki, Reykjanes, and Copahue, boiling point depth (Eq. (1)) was estimated by regression (Fig. 2). The effect of the regression scatter on the final reservoir temperature estimate was investigated by a Monte Carlo simulation (1000 realisations) (Robert and Casella, 2013), developed in Microsoft Excel; a boiling point depth was generated for each shallow temperature measurement by random selection from a normally distributed population. The normal distribution was modelled on the actual data; the mean of the population was set to the boiling point depth estimated from the regression (Fig. 2a and c), and standard deviation set to the standard error at that temperature (Fig. 2b and d).

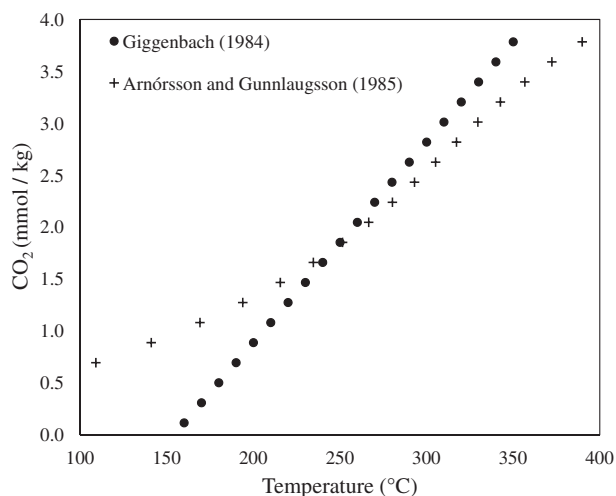


Fig. 3. Comparison of $T_{\text{CO}_2 \text{ Flux}}$ (Arnórsson and Gunnlaugsson, 1985; Eq. 3) and $T_{\text{CO}_2 \text{ Flux Gigg}}$ (Giggenbach, 1984; Eq. 4) for a range of CO_2 concentrations in surface vapour.

2.6. Methodology for determination of Biological Background CO_2 flux

A proportion of CO_2 flux measurements were collected in areas where a biological (background) CO_2 flux would be expected. Biological CO_2 flux in these areas was previously evaluated using statistical techniques (Copahue, Reykjanes) (Fridriksson et al., 2006; Chiodini et al., 2015), or ^{13}C isotope analysis (New Zealand systems) (Harvey et al., 2015b) (Table 1). Accordingly, biological flux values were subtracted from measurements prior to calculation of $T_{\text{CO}_2 \text{ Flux}}$. Negative CO_2 flux values (i.e. after subtraction) were disregarded.

Table 2
Summary of results.

Area	n^a	Survey Area (m ²)	$\text{CO}_2/\text{H}_2\text{O}^b$ (mmol/100 mol)	$\text{CO}_2/\text{H}_2\text{O}^b$ (log mmol/kg)	Mean $T_{\text{CO}_2 \text{ Flux}}^c$ (°C)	\pm^d (°C)	Mode(s) $T_{\text{CO}_2 \text{ Flux}}^e$ (°C)	Fig.
Tauhara	332	1.4E + 05	219	2.09	266	71	270	Fig. 5
Wairakei Outflow Areas	263	3.2E + 05	70	1.59	222	92	190, 230	Fig. 4
Wairakei Upflow Areas	148	2.0E + 05	135	1.88	249	83	270	Fig. 4
Reporoa	104	2.3E + 03	1027	2.76	314	97	290–330	Fig. 5
Rotokawa	1186	1.7E + 06	693	2.59	304	158	280, 320	Fig. 5
Ohaaki West	417	2.1E + 05	308	2.23	272	96	190, 260, 300	Fig. 6
Ohaaki East	386	3.4E + 05	446	2.39	287	96	280	Fig. 6
White Island	581	2.8E + 05	741	2.61	303	129	320	Fig. 6
Copahue	447	9.8E + 05	547	2.48	293	133	300	Fig. 6
Reykjanes 2004	167	1.50E + 05	310	2.24	276	96	270	Fig. 7
Reykjanes 2007	243	2.40E + 05	233	2.11	267	80	290	Fig. 7
All data 2004 & 2007	410		272	2.16	271	86	280	Fig. 7

^a Number of measurements in survey area.

^b $\text{CO}_2/\text{H}_2\text{O}$ ratio corresponding to the mean temperature.

^c Arithmetic mean of temperatures.

^d two standard deviations.

^e Temperature from histogram peak(s).

3. RESULTS

Soil CO_2 flux and shallow temperature results were converted to $T_{\text{CO}_2 \text{ Flux}}$ (°C) (Eq. (3)), summarised in Table 2, and plotted as histograms (Figs. 4–7). These summary statistics are based on 4274 measurements, from eight systems in New Zealand, Iceland and Argentina. Raw data is provided as a table within the Electronic Annex. Population mean temperatures range from 222 °C (Wairakei outflow) to 314 °C (Reporoa). Dominant histogram peak (mode) temperatures range from 230 °C (Wairakei outflow) to 320 °C (White Island).

For Rotokawa, White Island, Ohaaki, Reykjanes, and Copahue, boiling point depth (Eq. (1)) was estimated by regression (Fig. 2). The effect of the regression scatter on mean $T_{\text{CO}_2 \text{ Flux}}$ was investigated by a Monte Carlo simulation. For Rotokawa, White Island, Ohaaki, and Reykjanes, the simulation provided mean $T_{\text{CO}_2 \text{ Flux}}$ within 1 °C of the mean $T_{\text{CO}_2 \text{ Flux}}$ of actual data. For Copahue, the simulation was within 4 °C of actual data.

4. DISCUSSION

In this section, we compare deep reservoir temperatures measured from geothermal drill holes to mean and mode temperatures estimated from the proposed CO_2 geothermometer ($T_{\text{CO}_2 \text{ Flux}}$) (Table 3). The purpose is to show the reliability of the geothermometer. The accuracy of H_2O flux estimates and variability of $T_{\text{CO}_2 \text{ Flux}}$ are discussed.

4.1. Wairakei and Tauhara

Deep aquifer temperatures for the Wairakei outflow were interpreted from drill holes located outside of the Te Mihi area of the field. The Te Mihi steamfield is located

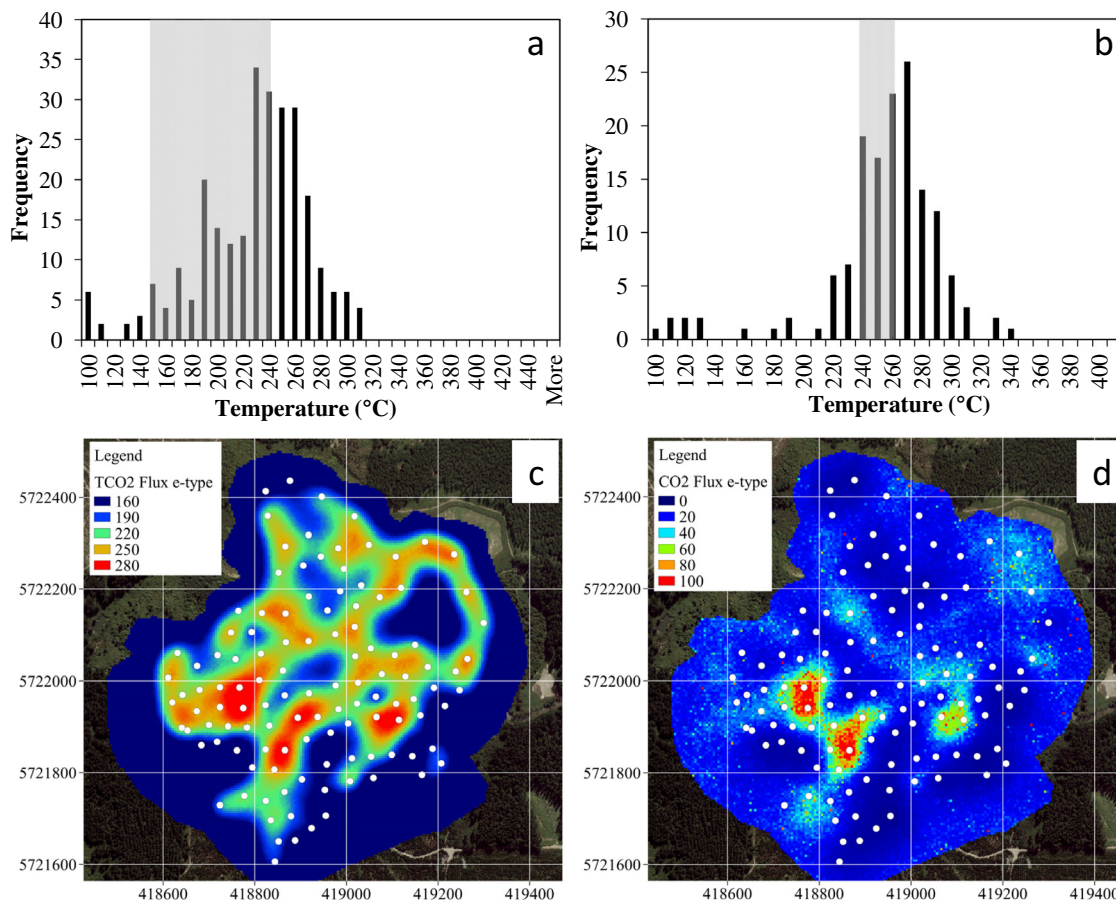


Fig. 4. $T_{CO_2 \text{ Flux}}$ histograms for (a) Wairakei outflow areas (Karapiti and Geysir Valley), and (b) Wairakei upflow areas (Wairoa Valley and Hot Hill). Shaded area shows range of measured temperatures from deep wells (Table 3). Interpolation (Sequential Gaussian Simulation) at Karapiti for (c) $T_{CO_2 \text{ Flux}}$ ($^{\circ}C$), and (d) $CO_2 \text{ Flux}$ ($g \text{ m}^{-2} \text{ d}^{-1}$). White points show measurement locations. Note: agreement between spatial distribution of (c) $T_{CO_2 \text{ Flux}}$ and (d) $CO_2 \text{ Flux}$ (d).

between the Upper Wairoa Valley and Hot Hill survey areas (Fig. 1a and b), and is regarded as the main upflow (Bixley et al., 2009). Temperatures for liquid-phase geothermal wells in outflow areas have a wide range (150–240 $^{\circ}C$), with temperatures increasing in proximity to Te Mihi (Bixley et al., 2009). This range of temperatures is consistent with the mean of $CO_2 \text{ flux}$ geothermometer data in this area ($\mu = 222 \text{ }^{\circ}C$) (Table 3). However, the distribution of $T_{CO_2 \text{ Flux}}$ values in the Wairakei outflow data (Geysir Valley and Karapiti; Fig. 1c and d) show a minor (190 $^{\circ}C$) and major (230 $^{\circ}C$) peak within the histogram (Fig. 4a). The presence of multiple peaks may indicate that separate aquifers are supplying steam and CO_2 in outflow areas, particularly Karapiti.

Previous studies have noted that steam and gas discharge at Karapiti originate from the main upflow zones at Wairakei (Allis, 1981; Glover et al., 2001); fluids flow laterally toward Karapiti, following fractures in the shallow upper surface of the Karapiti Rhyolite (Allis, 1981). Deep geothermal wells in the vicinity of Karapiti are comparatively cool (<200 $^{\circ}C$) (Allis, 1981). Accordingly, the presence of two

peaks in our data may reflect the presence of a deeper, cooler aquifer directly beneath Karapiti (minor peak), and the main upflow that is located near Te Mihi (major peak).

Deep aquifer temperatures for the Wairakei upflow zone were interpreted from drill holes located in the Te Mihi area of the field, and have remained stable at 240–265 $^{\circ}C$ since 1993 (Glover et al., 2001; Bixley et al., 2009). This temperature range is consistent with the mean ($\mu = 249 \text{ }^{\circ}C$), and close to the mode (270 $^{\circ}C$) of $T_{CO_2 \text{ Flux}}$ in the Wairakei upflow data (Hot Hill and the Upper Wairoa Valley; Fig. 1a and b) (Fig. 4b) (Table 3).

The spatial distribution of $T_{CO_2 \text{ Flux}}$ (Fig. 4c) and $CO_2 \text{ flux}$ (Fig. 4d) at Karapiti show close agreement. This shows that $CO_2 \text{ flux}$ dominates $H_2O \text{ flux}$ in the calculation of $T_{CO_2 \text{ Flux}}$. This is because $H_2O \text{ flux}$ for our dataset varies by ~ 1 order-of-magnitude, whereas $CO_2 \text{ flux}$ varies by 3–4 orders of magnitude. The single order-of-magnitude range of diffuse $H_2O \text{ fluxes}$ at Karapiti agrees with earlier reports at Karapiti (Hochstein and Bromley, 2005) and Solfatara (Italy) (Werner et al., 2006). The comparatively much wider range of $CO_2 \text{ fluxes}$ has been noted in

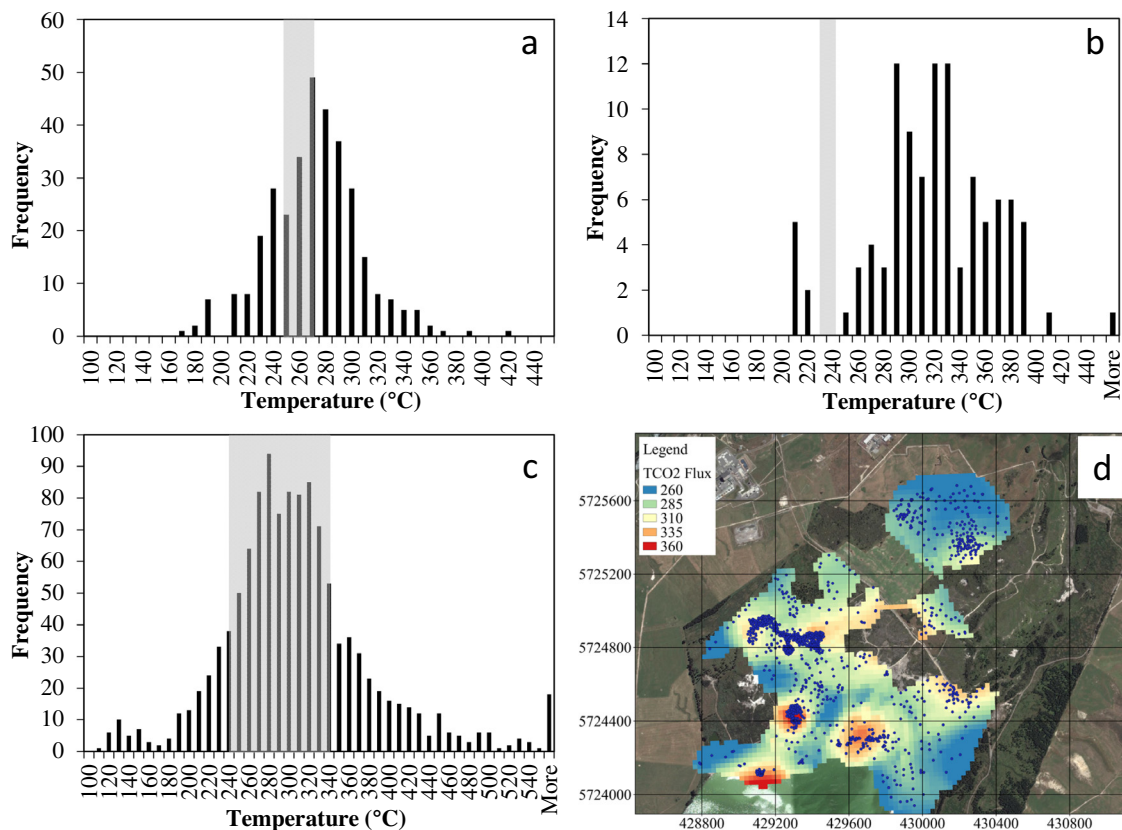


Fig. 5. $T_{CO_2 \text{ Flux}}$ histograms for (a) Tauhara (Pony Club), and (b) Reporoa (Opaheke), (c) Rotokawa, and (d) spatial distribution for Rotokawa ($^{\circ}C$): blue points show measurement locations. Shaded area shows range of measured temperatures from deep wells (Table 3). Note: $T_{CO_2 \text{ Flux}}$ reaches maximum near Lake Rotokawa (south of map) and decreases to north (interpolation by Ordinary Kriging). (For interpretation of the references to colour in this figure legend, the reader is referred to the web version of this article.)

numerous studies previously (e.g. Fridriksson et al., 2006; Werner and Cardellini, 2006; Bloomberg et al., 2012; Rissmann et al., 2012).

The deep aquifer temperature at Tauhara is assumed to be the average of measured temperatures from drill holes located either side of the survey area (TH1, 248 $^{\circ}C$ and TH3, 272 $^{\circ}C$). Neither TH1 nor TH3 has shown any significant temperature change since the 1970s (Rosenberg et al., 2010). The average of these values (260 $^{\circ}C$) is consistent with the mean and mode $T_{CO_2 \text{ Flux}}$ in this area (266 and 270 $^{\circ}C$, respectively) (Fig. 5a, Table 3).

An independent samples *t*-test was performed between the population of $T_{CO_2 \text{ Flux}}$ values of upflow areas at Wairakei ($\mu = 249$ $^{\circ}C$), and Tauhara ($\mu = 266$ $^{\circ}C$). The test was found to be statistically significant ($p < 0.05$). This result is consistent with higher measured well temperatures at the Tauhara survey area (Table 3), and with a previous interpretation that Tauhara has a separate, hotter upflow from Wairakei (280–300 $^{\circ}C$) (Rosenberg et al., 2010).

4.2. Rotokawa

Well data shows large chemical gradients from Rotokawa South (Lake Rotokawa) to Rotokawa North (Waikato River), with much higher concentrations of Cl, B,

Li, Cs and non-condensable gases (NCG) (predominantly CO_2) in the south. CO_2/Cl and B/Cl ratios are also higher in the south. Together with chloride-enthalpy mixing trends, the geochemical data suggests the main upflow occurs in the south of the field, possibly beneath Lake Rotokawa (Giggenbach, 1995; Winick et al., 2009; McNamara et al., 2016).

Well data identifies distinct deep (300–340 $^{\circ}C$) and intermediate depth aquifers (<300 $^{\circ}C$), separated by a smectite-rich clay zone. The distribution of $T_{CO_2 \text{ Flux}}$ at Rotokawa may be bimodal, with peaks at 280 $^{\circ}C$ and 320 $^{\circ}C$ (Fig. 5c) (Table 3), which may correlate with the intermediate and deep aquifers. The spatial distribution of $T_{CO_2 \text{ Flux}}$ shows a clear pattern of higher temperatures in the south, near Lake Rotokawa (Fig. 5d), consistent with previous interpretations of the main upflow in this area. The standard deviation for the Rotokawa population ($\mu = 304$ $^{\circ}C$) is the largest of all areas (2 standard deviations = 158 $^{\circ}C$), a consequence of the large temperature gradient between Lake Rotokawa and the north of the survey area.

4.3. Ohaaki

Well data shows Ohaaki West and East are geochemically distinct, and may have separate upflows. Previous

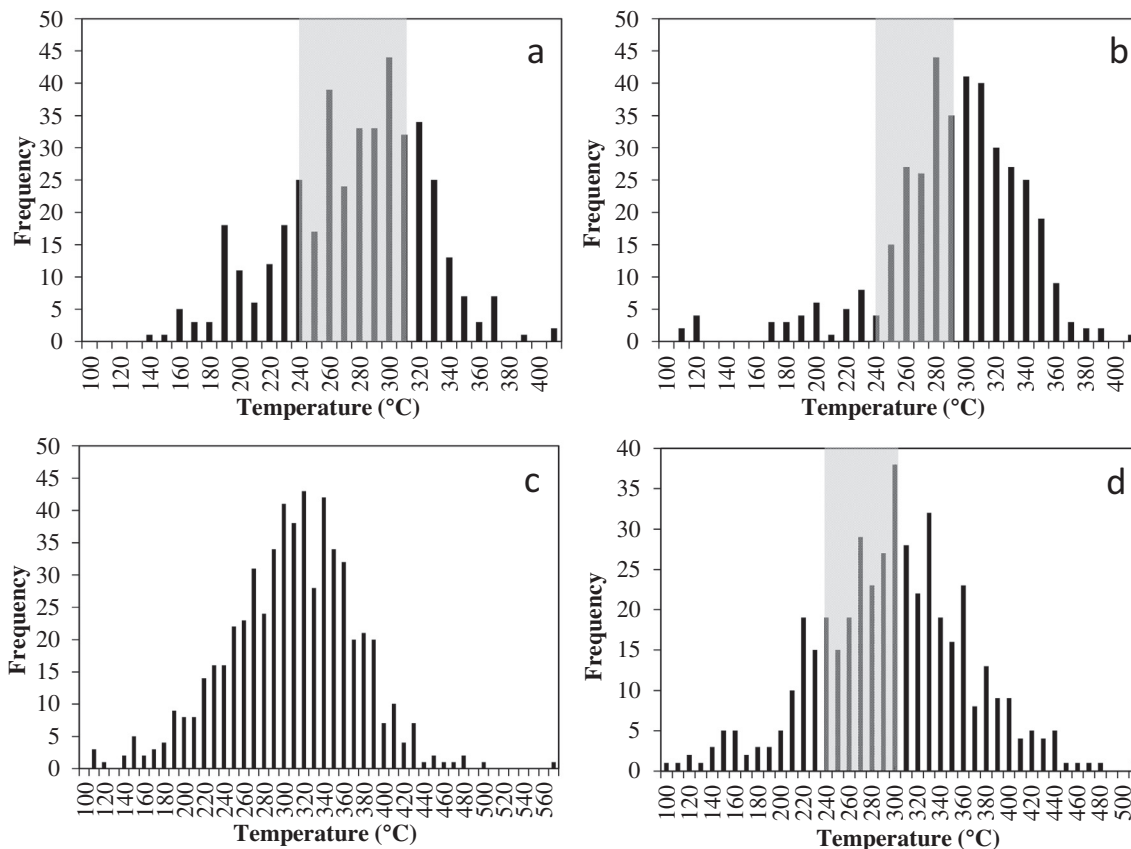


Fig. 6. $T_{CO_2 \text{ Flux}}$ histograms for (a) Ohaaki West, and (b) Ohaaki East, (c) White Island and (d) Copahue (all areas). Shaded area shows range of measured temperatures from deep wells (Note: most feed-zones at Ohaaki West exceed 240 °C) (Table 3).

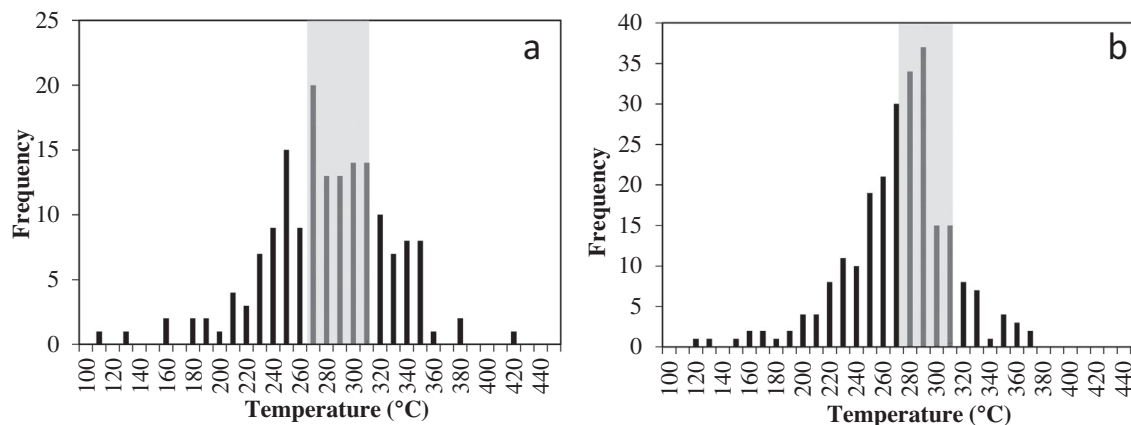


Fig. 7. $T_{CO_2 \text{ Flux}}$ histograms for Reykjanes (a) 2004, and (b) 2007. Shaded area shows range of measured temperatures from deep wells (Table 3).

authors have concluded that the East Bank has a more “magmatic” character than the West Bank, based on higher concentrations NCG (predominantly CO_2), and higher B/Cl ratios in the reservoir fluid (Giggenbach, 1989; Christenson et al., 2002; Rissmann et al., 2012); it was theorized that the East Bank fluid chemistry result from a more juvenile and shallower intrusive heat source (i.e.

younger and shallower than the West bank intrusive) (Christenson et al., 2002). More recently, other explanations for the distinctive geochemistry have been put forward, including a single deep parent fluid that diverges then undergoes secondary boiling (boiling of a shallow, CO_2 -rich, steam-heated aquifer) and dilution processes (Hedenquist, 1990; Mroczek et al., 2016).

Table 3
Aquifer temperatures versus CO₂ flux geothermometer temperatures.

System	Aquifer Temp (°C) ^a	$T_{\text{CO}_2 \text{ Flux}}$ (°C) ^b		Notes
		Mean	Mode(s)	
Tauhara	250–270	266	270	Deep aquifer temperatures in the survey area based on deep well data (Rosenberg et al., 2010)
Wairakei Outflow Areas	150–240	222	190, 230	Deep aquifer temperature from deep well data (Glover et al., 2001; Bixley et al., 2009; Sepulveda et al., 2012)
Wairakei Upflow Areas	240–260	249	270	
Reporoa	234	314	290–330	Deep aquifer is thought to have high CO ₂ based on one exploration well (RP1) (DSIR, 1967)
Rotokawa	240–300 (intermediate), 300–340 (deep)	304	280, 320	Deep and intermediate aquifer temperatures (Winick et al., 2009 and McNamara et al., 2016)
Ohaaki West	180–310	272	190, 260, 300	Measured temperatures from deep wells at major and secondary feed zones (Mroczek et al., 2016). The deep aquifer at Ohaaki is generally reported to be 300–310 °C (Hedenquist, 1990; Rissmann et al., 2012; Mroczek et al., 2016)
Ohaaki East	240–290	287	280	
White Island Copahue	High 240–300	303 293	320 300	Vapour core system (Giggenbach, 1987) Deep aquifer temperature from deep wells located 1–2 km from the survey areas (240–260 °C) (Chiodini et al., 2015), and gas geothermometry from fumaroles in the survey areas (250–300 °C) (Agusto et al., 2013)
Reykjanes (2004)	275–310	276	270	Deep aquifer temperature from deep wells in the survey area [Fig 2(b), Freedman et al. (2009)]
Reykjanes (2007)	275–310	267	290	

^a Temperature from deep well measurements.

^b Temperature from CO₂ flux geothermometer (mean and mode).

Well data from major and secondary feed-zones shows temperatures range from 180 to 310 °C on the West Bank, and 240–290 °C on the East Bank, increasing with depth (Mroczek et al., 2016) (Table 3). The distribution of $T_{\text{CO}_2 \text{ Flux}}$ at Ohaaki West (Fig. 1e) is tri-modal, with peaks at 190 °C, 260 °C, and a dominant peak at 300 °C (Fig. 6a), which may reflect the wide range of feed zone temperatures (180–310 °C). Most feed zones at Ohaaki West exceed 240 °C (Mroczek et al., 2016 – see Fig. 6 in that study). The distribution of $T_{\text{CO}_2 \text{ Flux}}$ at Ohaaki East (Fig. 1f) is unimodal (280 °C, Fig. 6b), which may reflect the narrower range of feed zone temperatures (240–290 °C) (Mroczek et al., 2016).

An independent samples *t*-test was performed between the population of $T_{\text{CO}_2 \text{ Flux}}$ values at Ohaaki West ($\mu = 272$ °C) and Ohaaki East ($\mu = 287$ °C). The test was found to be statistically significant ($p < 0.05$). The higher $T_{\text{CO}_2 \text{ Flux}}$ at Ohaaki East is consistent with previous observations of higher NCG, and interpretations of a more magmatic character for eastern reservoir fluids (Giggenbach, 1989; Christenson et al., 2002; Rissmann et al., 2012).

4.4. Reporoa

Only one deep well exists at Reporoa (RP-1), and is located within 100 m of the survey area. Measured temperatures for RP-1 peaked 234 °C (975 mMD) (Healy and Hochstein, 1973). However, the well discharged for only 5 h and was likely diluted by drilling fluids (Simpson and Bignall, 2016).

The well discharged fluids that were lower in chloride and lithium than nearby hot springs at Opaheke (DSIR, 1967;

Simpson and Bignall, 2016), which also suggests the well fluids were diluted, and/or the springs are supplied by deeper (and presumably hotter) fluids. Accordingly, deep temperatures beneath the Reporoa survey area are likely to be hotter than measured at RP-1. The $T_{\text{CO}_2 \text{ Flux}}$ histogram peak at Reporoa is poorly developed, but an emergent peak (290–330 °C, Fig. 5b), and high mean $T_{\text{CO}_2 \text{ Flux}}$ ($\mu = 314$ °C) indicates temperatures at depth may be considerably hotter than measured temperatures in RP-1. Reporoa has the smallest population size ($n = 104$) of all areas, which explains the poor development of the histogram.

4.5. White Island

White Island is an active volcano with no deep wells, but is inferred to host an acidic liquid geothermal reservoir surrounding a vapour-core at depth (Houghton and Nairn, 1991). It is a magmatic type hydrothermal system with numerous high temperature fumaroles (100–800 °C) (Hedenquist et al., 1993).

The distribution of $T_{\text{CO}_2 \text{ Flux}}$ at White Island is unimodal (320 °C, Fig. 6c), the highest of the systems considered in this study. At White Island, powerful magmatic CO₂ flows would be expected to penetrate or bypass the acidic liquid reservoir, especially during non-equilibrium eruptive events. Such a process would invalidate the $T_{\text{CO}_2 \text{ Flux}}$ geothermometer, which assumes temperature dependent water mineral equilibrium in neutral pH reservoir fluids. However, White Island is included in this study as it provides an example of how $T_{\text{CO}_2 \text{ Flux}}$ behaves in an acid-magmatic environment.

4.6. Copahue

Deep aquifer temperatures (240–300 °C) are based on deep wells located 1–2 km from the survey areas (240–260 °C) (Chiodini et al., 2015), and gas geothermometry from fumaroles in the survey areas (250–300 °C) (Agusto et al., 2013) (Table 3). However, Copahue is an active volcano with a main conduit and acid crater lake located ~6 km from the survey areas.

The distribution of $T_{\text{CO}_2 \text{ Flux}}$ at Copahue is unimodal (300 °C, Fig. 6d), at the top of the range of aquifer temperatures in the survey area based on fumarole geothermometry (240–300 °C).

4.7. Reykjanes

The 2004 and 2007 $T_{\text{CO}_2 \text{ Flux}}$ histograms for Reykjanes are both unimodal (270 and 290 °C respectively, Fig. 7). The apparent change in deep reservoir temperature at Reykjanes may result from an increase in measured well enthalpy that occurred over the same period. The enthalpy increase was due to commencement of exploitation of the field, with associated pressure decline and boiling. Between 2004 and 2008, the discharge enthalpy of deep production wells increased from 1210–1400 kJ/kg (liquid enthalpy at 275–310 °C) to 1450–1950 kJ/kg in 2008, while both surface steam and CO₂ fluxes increased rapidly during this period (Fridriksson et al., 2010).

In contrast to modal $T_{\text{CO}_2 \text{ Flux}}$, mean $T_{\text{CO}_2 \text{ Flux}}$ temperatures actually declined slightly over the same period (276–267 °C) (Table 2, Fig. 7). An independent samples *t*-test performed between the 2004 population of $T_{\text{CO}_2 \text{ Flux}}$ values at Reykjanes ($\mu = 276$ °C), and the 2007 population ($\mu = 267$ °C), was statistically significant ($p < 0.05$) (an independent *t*-test was utilised because the 2004/2007 measurements were not paired). Deep aquifer temperatures from wells in the survey area range from 275 to 310 °C (Freedman et al., 2009; Fig. 2b in that study) (Table 3), and average ~290 °C (Fridriksson et al., 2006).

4.8. Accuracy of H₂O flux estimates

All H₂O flux estimates are based on Eq. (1), an empirical relation based on calorimetry measurements made at the Wairakei and Tauhara thermal areas. Soils in these and the other TVZ survey areas (Rotokawa, Ohaaki, Reporoa and White Island) are composed of rhyolitic tephra (mostly pumice) (Pullar et al., 1973), variably altered to clay by hydrothermal activity (Hochstein and Bromley, 2005; Rissmann, 2010; Bloomberg et al., 2012). For this reason, and because ambient climatic effects will be similar, we assume Eq. (1) provides an accurate measure of heat flux for TVZ soils. This assumption is supported by a previous study that utilised Eq. (1) to assess heat flux from steam heated ground at Ohaaki (Rissmann, 2010).

Soils at Reykjanes and Copahue are also comprised of hydrothermally altered volcanics, and inferred reservoir temperatures in both areas are within the range $T_{\text{CO}_2 \text{ Flux}}$ estimates (Table 3). This suggests Eq. (1) is also appropriate for estimates of H₂O flux in these areas. However,

additional studies are required (in areas with deep well temperature data) to confirm Eq. (1) and $T_{\text{CO}_2 \text{ Flux}}$ are generally applicable outside of the TVZ.

For Rotokawa, White Island, Ohaaki, Reykjanes, and Copahue, boiling point depths (Eq. (1)) were not determined by soil temperature profiles, but estimated from temperature at a single depth (see regression equations in Fig. 2). The effect of the regression scatter on the mean $T_{\text{CO}_2 \text{ Flux}}$ was investigated by a Monte Carlo simulation and found to be minimal (within 1–4 °C of actual data). This result suggests that mean $T_{\text{CO}_2 \text{ Flux}}$ is insensitive to random error in the calculation of H₂O flux.

It must be noted that the regression equations are derived from shallow temperature data collected in the TVZ, in the summer months (ambient air temperature ~20 °C). While the regressions are appropriate for estimating boiling point depth in other TVZ systems also surveyed in the summer (i.e. Rotokawa, White Island, Ohaaki), they may be less so for Reykjanes, and Copahue where the climate is significantly cooler. The effect of the cooler conditions at Reykjanes and Copahue (relative to the TVZ) are unknown but may be significant. Further work is required to determine the applicability of regression equations presented here in cooler climates. We recommend that future studies collect temperature profile data to accurately determine boiling point depth.

4.9. Causes of variability of $T_{\text{CO}_2 \text{ Flux}}$ within the histogram

Our results show surface CO₂ flux and shallow temperature measurements can provide an estimate of the deep geothermal reservoir temperature. However, $T_{\text{CO}_2 \text{ Flux}}$ data present as variable, normally distributed datasets. Conceptual models for systems considered here (excluding White Island) assume the existence of discrete, liquid-phase reservoirs at depth. In all cases, the range of temperatures reported for each system is narrower than the corresponding range of $T_{\text{CO}_2 \text{ Flux}}$ values (Table 1). This suggests the variability in our datasets is not determined by the variability in the reservoir, but random processes occurring (i) in the subsurface, and/or (ii) measurement error.

Firstly, it is possible the variability results from heterogeneity in the permeability of subsurface materials that comprise the thermal area. For example, surficial “alteration crusts”, thin crusts of fumarolic sublimates and/or alteration, were previously reported to cause large variations in CO₂ flux in thermal areas (Chiodini et al., 1996). Alteration crusts and impermeable thermal clays were also noted to effect CO₂ flux in this study (Tauhara, Wairakei and Reporoa thermal areas), and in previous studies at Rotokawa and White Island (Bloomberg et al., 2012). CO₂ flux was observed to vary by orders of magnitude over small distances (~1 m) where crust was present. Heterogeneity from surface crusts, or other obstructions, might affect the quantification of CO₂ and H₂O fluxes in different ways, as H₂O vapour is subject to condensation at the soil-atmosphere interface.

Let us consider an example relating to the low tail of the $T_{\text{CO}_2 \text{ Flux}}$ histograms (Figs. 4–7). Here, the measurements are affected by restricted near-surface permeability, which

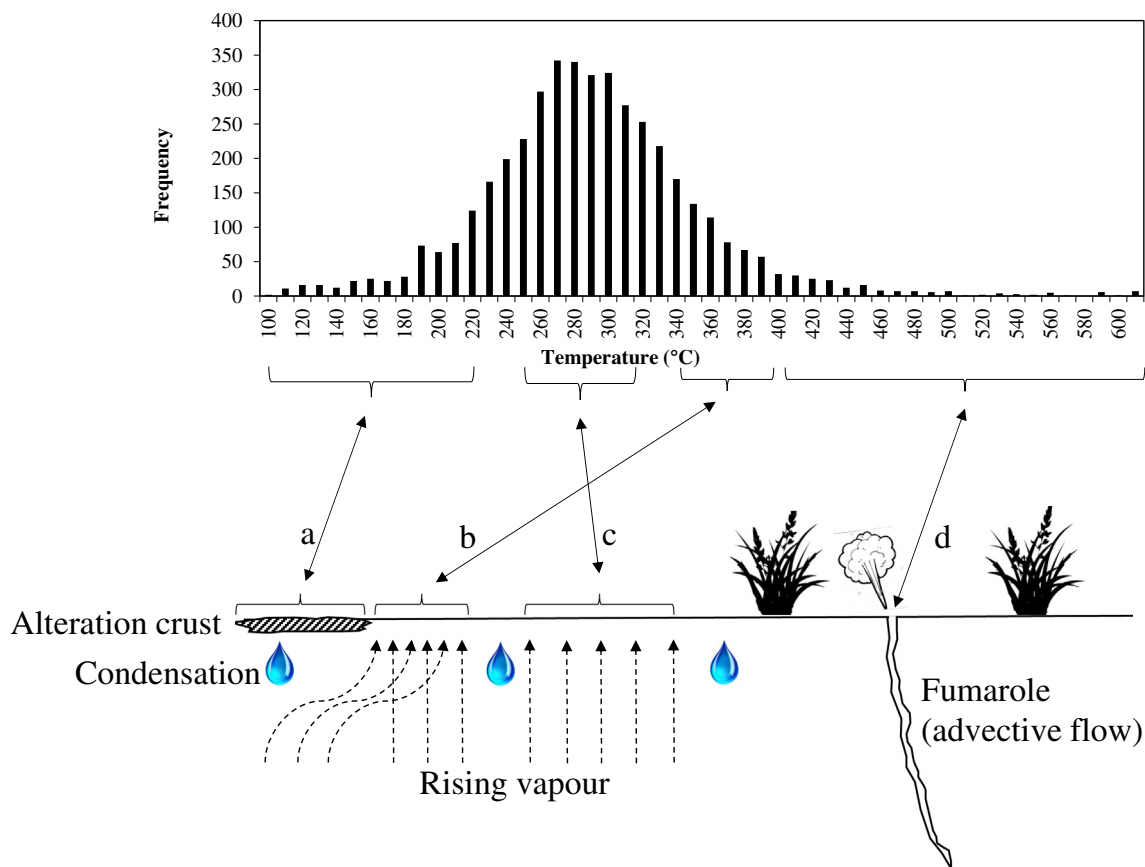


Fig. 8. Causes of variability of $T_{\text{CO}_2 \text{ Flux}}$ within a thermal area. (a) Rising vapour encounters a near surface impermeable layer (e.g. alteration crust), (b) re-routed CO_2 converges with adjacent vapor stream and enters the atmosphere. This creates localized areas of anomalously high CO_2 flux, (c) composition of vapour reflects adiabatic boiling of the reservoir, and (d) very high CO_2 fluxes and correspondingly high $T_{\text{CO}_2 \text{ Flux}}$ are expected where vapour flows advectively from the system.

causes low vapour flux. For example, the rising vapour (mix of CO_2 and H_2O in the gas phase) encounters a near surface, impermeable layer (Fig. 8a). The H_2O component within the vapour is blocked and may condense, releasing heat by conduction. The conductive heat loss is detected by our probe and gives a large denominator in the $\text{CO}_2/\text{H}_2\text{O}$ ratio (low $T_{\text{CO}_2 \text{ Flux}}$). The CO_2 is also blocked, but cannot condense. Instead, it is re-routed to surface elsewhere; the CO_2 does not pass into the accumulation chamber of the instrument, and is not detected, which gives a small numerator (low $T_{\text{CO}_2 \text{ Flux}}$).

Simultaneously, this process may contribute to measurements in high tail, as re-routed CO_2 converges with the adjacent vapor stream and enters the atmosphere. This creates localized areas of anomalously high CO_2 flux (Fig. 8b), which gives a relatively large numerator (high $T_{\text{CO}_2 \text{ Flux}}$).

Very high values of $T_{\text{CO}_2 \text{ Flux}}$ may be expected where vapour flows advectively (high numerator) from the system (e.g. fumaroles or small vents). Such point-source CO_2 discharges, are analogous to including a gold nugget in a bulk metallurgical assay; in geostatistical terminology, this is the “pure nugget” effect (Armstrong, 1998). Importantly, water vapour may escape condensation and flow to the atmo-

sphere without releasing much heat to the soil (advective heat loss), so there is no nugget in the denominator (Fig. 8d).

Although shallow temperature measurements were made immediately adjacent to the CO_2 flux meter’s accumulation chamber, this may not provide an estimate of H_2O flux that represents the area beneath the chamber. This provides another mechanism by which high spatial variability can randomly affect our results. The magnitude of this error will depend on the spatial variability of the vapour flux; it can be considered part of the nugget effect (Armstrong, 1998). Additional high-density surveying (i.e. sub-meter scale measurement spacing) might resolve these effects, but is beyond the scope of this investigation.

The above processes represent extreme cases, and may give rise to the histogram tails. More commonly, we expect estimates of the relative proportion of H_2O and CO_2 in the rising vapour to reflect adiabatic boiling of the reservoir at depth (Fig. 8c). In summary, variability shown in the histogram does not represent variability in deep reservoir temperature. Instead, it results from large variations in the vapour flux, caused by spatially variable permeability in near-surface materials.

5. CONCLUSIONS

Here we have compared geothermometry based on measurements of CO₂ flux and shallow temperature on steaming ground ($T_{\text{CO}_2 \text{ Flux}}$), with measured and inferred reservoir temperatures from eight geothermal systems in New Zealand (6), Iceland (1) and Argentina (1). Survey measurements from steaming ground provided populations of reservoir temperatures that were described by normal statistical measures (mean, mode and standard deviation).

Mean $T_{\text{CO}_2 \text{ Flux}}$ estimates fall within the range of measured reservoir temperatures for Wairakei, Tauhara, Rotokawa, Ohaaki, Reykjanes and Copahue. At White Island, strong CO₂ flows are released from magma, rise, and penetrate the acidic liquid reservoir, particularly during eruptive events. The $T_{\text{CO}_2 \text{ Flux}}$ geothermometer relies on mineral–water equilibrium in neutral pH reservoir fluids, and would not be reliable in such an active and acidic environment.

We propose that the $T_{\text{CO}_2 \text{ Flux}}$ geothermometer provides an estimate of reservoir temperature that avoids the problems of limited sample size inherent to current water and gas geothermometers. We based $T_{\text{CO}_2 \text{ Flux}}$ on the fumarole CO₂ geothermometer of Arnórsson and Gunnlaugsson (1985). However, it is equally possible to adapt the full equilibrium CO₂ geothermometer of Giggenbach (1984) for this purpose. These approaches will provide similar results (<10 °C difference) for reservoir temperatures in the range 200–300 °C.

The distribution of $T_{\text{CO}_2 \text{ Flux}}$ in some areas is multimodal (Wairakei, Ohaaki, Rotokawa), which may indicate surface thermal areas are supplied by vapour from distinct aquifers. At Wairakei and Rotokawa, the areas of highest $T_{\text{CO}_2 \text{ Flux}}$ are consistent with the location of upflows from existing conceptual models. Mean $T_{\text{CO}_2 \text{ Flux}}$ at Reporoa (310 °C) is high, which indicates Reporoa has a separate upflow from Waiotapu; an outflow from Waiotapu would not be expected to have such high temperature. Upper and lower tails in the $T_{\text{CO}_2 \text{ Flux}}$ histogram may result from large variations in the vapour flux, caused by spatially variable permeability in near-surface materials.

ACKNOWLEDGMENTS

We would like to acknowledge support for this research by GNS Science and The University of Auckland.

APPENDIX A. SUPPLEMENTARY MATERIAL

Supplementary data associated with this article can be found, in the online version, at <http://dx.doi.org/10.1016/j.gca.2017.06.025>.

REFERENCES

Agusto M., Tassi F., Caselli A. T., Vaselli O., Rouwet D., Capaccioni B., Caliro F., Chiodini G. and Darrah T. (2013) Gas geochemistry of the magmatic-hydrothermal fluid reservoir in the Copahue-Caviahue Volcanic Complex (Argentina). *J. Volcanol. Geotherm. Res.* **257**, 44–56.

Allis R. G. (1981) Changes in heat flow associated with exploitation of Wairakei geothermal field, New Zealand. *New Zeal. J. Geol. Geophys.* **24**, 1–19.

Ármansson H. (2016) The fluid geochemistry of Icelandic high temperature geothermal areas. *Appl. Geochem.* **66**, 14–64.

Armstrong M. (1998) *Basic Linear Geostatistics*. Springer Science & Business Media.

Arnórsson S. (1978) Major element chemistry of the geothermal sea-water at Reykjanes and Svartsengi, Iceland. *Mineral. Mag.* **42**, 209.

Arnórsson S. and Gunnlaugsson E. (1985) New gas geothermometers for geothermal exploration—calibration and application. *Geochem. Cosmochim. Acta* **49**, 1307–1325.

Arnórsson S. (1985) The use of mixing models and chemical geothermometers for estimating underground temperatures in geothermal systems. *J. Volcanol. Geotherm. Res.* **23**, 299–335.

Arnórsson, S., Fridriksson, T., and Gunnarsson, I. (1998) Gas chemistry of the Krafla Geothermal field, Iceland. In Proceedings of the 9th International Symposium Water-Rock Interaction, WRI-9 (eds. G. B. Arehart and J. R. Hulston). pp. 613–616.

Arnórsson S., Bjarnason J. Ö., Giroud N., Gunnarsson I. and Stefánsson A. (2006) Sampling and analysis of geothermal fluids. *Geofluids* **6**, 203–216.

Bibby H. M., Bennie S. L., Stagpoole V. M. and Caldwell T. G. (1994) Resistivity structure of the Waimangu, Waiotapu, Waikite and Reporoa geothermal areas, New Zealand. *Geothermics* **23**, 445–471.

Bixley P. F., Clotworthy A. W. and Mannington W. I. (2009) Evolution of the Wairakei geothermal reservoir during 50 years of production. *Geothermics* **38**, 145–154.

Bloomberg, S., Rissmann, C., Mazot, A., Oze, C., Horton, T., Gravley, D., Kennedy, B., Werner, C., Christenson, B., and Pawson J. (2012) Soil gas flux exploration at the Rotokawa geothermal field and White Island, New Zealand. *Proceedings, Thirty-Sixth Workshop on Geothermal Reservoir Engineering*.

Bloomberg S., Werner C., Rissmann C., Mazot A., Horton T., Gravley D., Kennedy B. and Oze C. (2014) Soil CO₂ emissions as a proxy for heat and mass flow assessment, Taupō Volcanic Zone, New Zealand. *Geochem. Geophys. Geosyst.* **15**, 4885–4904.

Brombach T., Hunziker J. C., Chiodini G., Cardellini C. and Marini L. (2001) Soil diffuse degassing and thermal energy fluxes from the southern Lakki plain, Nisyros (Greece). *Geophys. Res. Lett.* **28**, 69–72.

Bromley, C. J., and Hochstein, M. P. (2005) Heat discharge of steaming ground at Karapiti (Wairakei), New Zealand. *Proc. World Geotherm. Congr.* **3rd**.

Browne P. R. L. and Ellis A. J. (1970) The Ohaki-Broadlands hydrothermal area, New Zealand; mineralogy and related geochemistry. *Am. J. Sci.* **269**, 97–131.

Chiodini G., Cioni R., Guidi M., Raco B. and Marini L. (1998) Soil CO₂ flux measurements in volcanic and geothermal areas. *Appl. Geochem.* **13**, 543–552.

Chiodini G., Frondini F. and Raco B. (1996) Diffuse emission of CO₂ from the Fossa crater, Vulcano Island (Italy). *Bull. Volcan.* **58**, 41–50.

Chiodini G. and Marini L. (1998) Hydrothermal gas equilibria: the H₂–OH₂–CO₂–CO–CH₄ system. *Geochem. Cosmochim. Acta* **62**, 2673–2687.

Chiodini G., Granieri D., Avino R., Caliro S., Costa A. and Werner C. (2005) Carbon dioxide diffuse degassing and estimation of heat release from volcanic and hydrothermal systems. *J. Geophys. Res.: Sol. Ear.* **110**.

Chiodini G., Cardellini C., Lamberti M. C., Agusto M., Caselli A., Liccioli C., Tamburello G., Tassi F., Vaselli O. and Caliro S.

- (2015) Carbon dioxide diffuse emission and thermal energy release from hydrothermal systems at Copahue-Caviahue Volcanic Complex (Argentina). *J. Volcanol. Geotherm. Res.* **304**, 294–303.
- Christenson B. W., Mroczek E. K., Kennedy B. M., Van Soest M. C., Stewart M. K. and Lyon G. (2002) Ohaaki reservoir chemistry: characteristics of an arc-type hydrothermal system in the Taupō Volcanic Zone. *New Zeal. J. Volcanol. Geotherm. Res.* **115**, 53–82.
- Dawson G. B. (1964) The nature and assessment of heat flow from hydrothermal areas. *New Zeal. J. Geol. Geophys.* **7**, 155–171.
- DSIR (1967) Chemistry of Hole 1 Reporoa (RP-1). Chemistry Division Report, DSIR. CD.118/12 – RGB/47 AJE.
- Fournier R. O. (1977) Chemical geothermometers and mixing models for geothermal systems. *Geothermics* **5**, 41–50.
- Freedman A. J., Bird D. K., Arnórsson S., Fridriksson T., Elders W. A. and Fridleifsson G. Ó. (2009) Hydrothermal minerals record CO₂ partial pressures in the Reykjanes geothermal system, Iceland. *Amer. J. Sci.* **309**, 788–833.
- Fridriksson T., Kristjánsson B. R., Ármannsson H., Margrétardóttir E., Ólafsdóttir S. and Chiodini G. (2006) CO₂ emissions and heat flow through soil, fumaroles, and steam heated mud pools at the Reykjanes geothermal area, SW Iceland. *Appl. Geochem.* **21**, 1551–1569.
- Fridriksson, T., Oladottir, A. A., Jonsson, P., and Eyjolfssdottir, E. I. (2010) The response of the Reykjanes geothermal system to 100 MWe power production: fluid chemistry and surface activity. *World Geotherm. Congr. 4th*.
- Giggenbach W. F. (1980) Geothermal gas equilibria. *Geochem. Cosmochim. Acta* **44**, 2021–2032.
- Giggenbach W. F. (1981) Geothermal mineral equilibria. *Geochem. Cosmochim. Acta* **45**, 393–410.
- Giggenbach W. F. (1984) Mass transfer in hydrothermal alteration systems—a conceptual approach. *Geochem. Cosmochim. Acta* **48**, 2693–2711.
- Giggenbach W. (1987) Redox processes governing the chemistry of fumarolic gas discharges from White Island, New Zealand. *Appl. Geochem.* **2**, 143–161.
- Giggenbach W. F. (1988) Geothermal solute equilibria. derivation of Na-K-Mg-Ca geothermometers. *Geochem. Cosmochim. Acta* **52**, 2749–2765.
- Giggenbach, W. F. (1989) The chemical and isotopic position of the Ohaaki field within the Taupo Volcanic Zone. In Proc. New Zeal. Geotherm. Workshop, 11th (eds. P. R. L. Browne and K. Nicholson).
- Giggenbach W. F. (1995) Variations in the chemical and isotopic composition of fluids discharged from the Taupo Volcanic Zone, New Zealand. *J. Volcanol. Geotherm. Res.* **68**, 89–116.
- Giggenbach W., Shinohara H., Kusakabe M. and Ohba T. (2003) Formation of acid volcanic brines through interaction of magmatic gases, seawater, and rock within the White Island volcanic-hydrothermal system. *New Zeal. Spec. Publ. Soc. Econ. Geol.* **10**, 19–40.
- Glover R. B., Mroczek E. K. and Finlayson J. B. (2001) Fumarolic gas chemistry at Wairakei, New Zealand, 1936–1998. *Geothermics* **30**, 511–525.
- Glover R. B. and Mroczek E. K. (2009) Chemical changes in natural features and well discharges in response to production at Wairakei, New Zealand. *Geothermics* **38**, 117–133.
- Harvey C. C. and Browne P. R. (1991) Mixed-layer clay geothermometry in the Wairakei geothermal field, New Zealand. *Clays Clay Min.* **39**(6), 614–621.
- Harvey M. C., Rowland J. V., Chiodini G., Rissmann C. F., Bloomberg S., Hernández P. A., Mazot A., Viveiros F. and Werner C. (2015a) Heat flux from magmatic hydrothermal systems related to availability of fluid recharge. *J. Volcanol. Geotherm. Res.* **302**, 225–236.
- Harvey, M. C., Zygadlo, M., and Dwivedi, A. (2015b) Use of isotopic analysis to distinguish between biological and geothermal soil CO₂ flux at Tauhara and Te Mihi geothermal areas. *Proc. New Zeal. Geotherm. Workshop, 37th*.
- Hatherton T., Macdonald W. J. P. and Thompson G. E. K. (1966) Geophysical methods in geothermal prospecting in New Zealand. *Bull. Volcanologique* **29**, 485–497.
- Healy J. and Hochstein M. P. (1973) Horizontal flow in hydrothermal systems. *J. Hydrol. New Zeal.* **12**, 71–82.
- Hedenquist J. W. (1990) The thermal and geochemical structure of the Broadlands-Ohaaki geothermal system, New Zealand. *Geothermics* **19**, 151–185.
- Hedenquist J. W., Simmons S. F., Giggenbach W. F. and Eldridge C. S. (1993) White Island, New Zealand, volcanic-hydrothermal system represents the geochemical environment of high-sulfidation Cu and Au ore deposition. *Geology* **21**, 731–734.
- Henley R. W., Truesdell A. H., Barton P. B. and Whitney J. A. (1974) .
- Hernández P. A., Pérez N. M., Fridriksson T., Egbert J., Ilyinskaya E., Thárhallsson A., Ívarsson G., Gíslason G., Gunnarsson I. and Jónsson B. (2012) Diffuse volcanic degassing and thermal energy release from Hengill volcanic system, Iceland. *Bull. Volcan.* **74**, 2435–2448.
- Hochstein M. P. and Bromley C. J. (2005) Measurement of heat flux from steaming ground. *Geotherm.* **34**, 131–158.
- Houghton B. and Nairn I. (1991) The 1976–1982 Strombolian and phreatomagmatic eruptions of White Island, New Zealand: eruptive and depositional mechanisms at a ‘wet’ volcano. *Bull. Volcanol.* **54**, 25–49.
- McNamara D. D., Sewell S., Buscarlet E. and Wallis I. C. (2016) A review of the Rotokawa Geothermal Field, New Zealand. *Geothermics* **59**, 281–293.
- Mroczek E. K., Milicich S. D., Bixley P. F., Sepulveda F., Bertrand E. A., Soengkono S. and Rae A. J. (2016) Ohaaki geothermal system: Refinement of a conceptual reservoir model. *Geothermics* **59**, 311–324.
- Pullar W. A., Birrell K. S. and Heine J. C. (1973) Named tephra and tephra formations occurring in the central North Island, with notes on derived soils and buried paleosols. *New Zeal. J. Geol. Geophys.* **16**, 497–518.
- Risk G. F., Caldwell T. G. and Bibby H. M. (1994) Deep resistivity surveys in the Waiotapu-Waikite-Reporoa region, New Zealand. *Geothermics* **23**, 423–443.
- Rissmann, C. F. W., (2010) Using surface methods to understand the Ohaaki Hydrothermal Field, Taupo Volcanic Zone, New Zealand. In PhD Thesis at the Department of Geological Sciences. University of Canterbury.
- Rissmann C., Christenson B., Werner C., Leybourne M., Cole J. and Gravley D. (2012) Surface heat flow and CO₂ emissions within the Ohaaki hydrothermal field, Taupō Volcanic Zone, New Zealand. *Appl. Geochem.* **27**, 223–239.
- Robert C. and Casella G. (2013) *Monte Carlo Statistical Methods*. Springer Science and Business Media.
- Rowland J. V. and Sibson R. H. (2004) Structural controls on hydrothermal flow in a segmented rift system, Taupō Volcanic Zone, New Zealand. *Geofluids* **4**, 259–283.
- Rosenberg M. D., Bignall G. and Rae A. J. (2009) The geological framework of the Wairakei-Tauhara geothermal system, New Zealand. *Geothermics* **38**, 72–84.
- Rosenberg, M., Wallin, E., Bannister, S., Bourguignon S., Sherburn, S., Jolly, G., Mroczek, E., Milicich, S., Graham, D., Bromley, C., Reeves, R., Bixley, P., Clothworthy, A., Carey, B., Climo, M., and Links, F. (2010) Tauhara Stage II Geothermal Project: Geo-Science report. In: GNS Science Consultancy

- Report 2010/138, February, 2010, <http://www.contactenergy.co.nz/aboutus/pdf/environmental/P3GeoscienceReport.pdf>.
- Sepúlveda F., Rosenberg M. D., Rowland J. V. and Simmons S. F. (2012) Kriging predictions of drill-hole stratigraphy and temperature data from the Wairakei geothermal field, New Zealand: Implications for conceptual modeling. *Geothermics* **42**, 13–31.
- Simpson M. P. and Bignall G. (2016) Undeveloped high-enthalpy geothermal fields of the Taupō Volcanic Zone, New Zealand. *Geothermics* **59**, 325–346.
- Stefánsson A. and Arnórsson S. (2002) Gas pressures and redox reactions in geothermal fluids in Iceland. *Chem. Geol.* **190**, 251–271.
- Steiner, A. (1977) The Wairakei geothermal area, North Island, New Zealand: its subsurface geology and hydrothermal rock alteration (No. 90). New Zealand Dept. of Scientific and Industrial Research.
- Werner, C. A., Hochstein, M. P., and Bromley, C.J. (2004) CO₂-flux of steaming ground at Karapiti, Wairakei. *Proc. New Zeal. Geotherm. Workshop*. 26th.
- Werner C. and Cardellini C. (2006) Comparison of carbon dioxide emissions with fluid upflow, chemistry, and geologic structures at the Rotorua geothermal system, New Zealand. *Geothermics* **35**, 221–238.
- Werner C., Chiodini G., Granieri D., Caliro S., Avino R. and Russo M. (2006) Eddy covariance measurements of hydrothermal heat flux at Solfatara volcano, Italy. *Earth Planet. Sci. Lett.* **244**, 72–82.
- Wilson C. J. and Rowland J. V. (2016) The volcanic, magmatic and tectonic setting of the Taupō Volcanic Zone, New Zealand, reviewed from a geothermal perspective. *Geothermics* **59**, 168–187.
- Winick, J., Powell, T., and Mroczek, E. (2009) The natural state chemistry of the Rotokawa reservoir. *Proc. New Zeal. Geotherm. Workshop*, 31st.

Associated editor: Edward M. Ripley